CHEMISTRY
A EUROPEAN JOURNAL

DOI: 10.1002/chem.201000546

VIP

Formation of Superoxo Species by Interaction of O_2 with Na Atoms Deposited on MgO Powders: A Combined Continuous-Wave EPR (CW-EPR), Hyperfine Sublevel Correlation (HYSCORE) and DFT Study

Francesco Napoli,[a] Mario Chiesa,*[a] Elio Giamello,[a] Gloria Preda,[b]
Cristiana Di Valentin,[b] and Gianfranco Pacchioni[b]

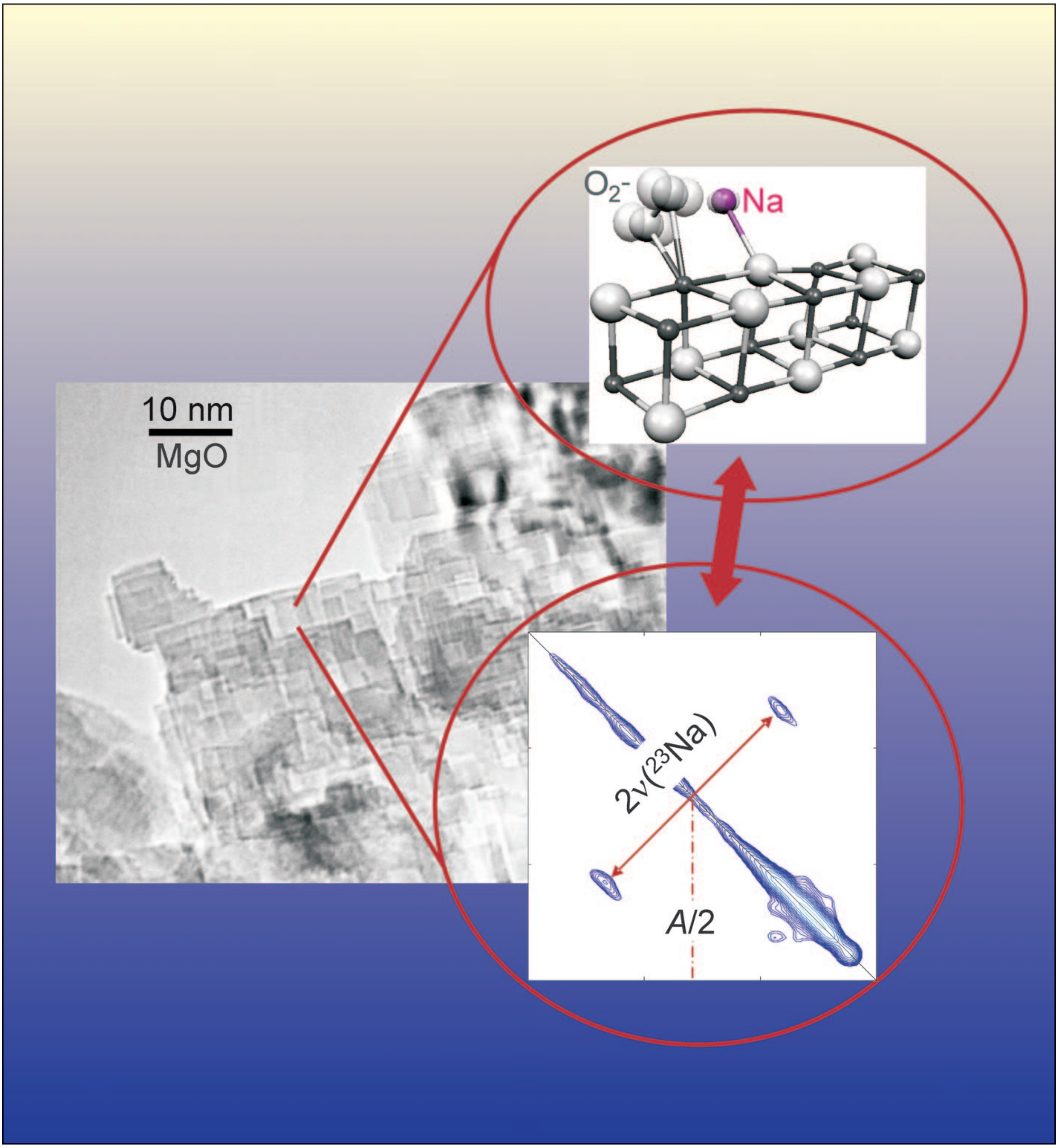

Abstract: The formation of O_2^- radical anions by contact of O_2 molecules with a Na pre-covered MgO surface is studied by a combined EPR and quantum chemical approach. Na atoms deposited on polycrystalline MgO samples are brought into contact with O_2. The typical EPR signal of isolated Na atoms disappears when the reaction with O_2 takes place and new paramagnetic species are observed, which are attributed to different surface-stabilised O_2^- radicals. Hyperfine sublevel correlation (HYSCORE) spectroscopy allows the superhyperfine interaction tensor of $O_2^-Na^+$ species to be determined, demonstrating the direct coordination of the O_2^- adsorbate to surface Na^+ cations. DFT calculations enable the structural details of the formed species to be determined. Matrix-isolated alkali superoxides are used as a standard to enable comparison of the formed species, revealing important and unexpected contributions of the MgO matrix in determining the electronic structure of the surface-stabilised $Na^+-O_2^-$ complexes.

Keywords: density functional calculations · EPR spectroscopy · magnesium oxide · superoxide · surface chemistry

Introduction

The interaction of alkali metal atoms with the surface of insulating oxides[1,2,3] and their subsequent reactivity towards gas-phase molecules[4] has attracted our interest in recent years because these systems represent well-defined models of activation of adsorbed molecules by effect of an electron transfer.

Alkali metal atoms can be stabilised at the surface of alkaline earth metal oxides as isolated atoms. These atoms are bound to morphological defects, in particular, cationic edges, reverse edges and reverse corners, and their valence electron is strongly polarised by the interaction with the substrate.[1] This bonding mechanism implies that no charge transfer occurs from the metal to the surface, and the alkali atoms remain essentially neutral.[3] Still, the interaction with the surface considerably lowers the ionisation potential of the deposited alkali atoms compared with the free atoms, an effect that is expected to favour the electron transfer to adsorbed molecular species. We recently reported that such an electron transfer occurs in the case of K atoms deposited on MgO towards the CO_2 molecule, leading to surface-stabilised CO_2^- radical anions.[4] In this paper we explore the reactivity of oxygen towards Na atoms deposited on the surface of MgO.

Molecular oxygen, in addition to the usual $^3\Sigma_g^-$ paramagnetic ground state, exhibits a variety of activated forms, among which superoxide O_2^- and peroxide O_2^{2-} states are particularly relevant in a number of phenomena taking place at gas–solid and liquid–solid interfaces including catalytic oxidation as well as biochemical processes.[5,6,7]

The chemistry of oxygen species at solid surfaces has attracted the attention of several research groups over the years owing to its relevance in various fields of modern science such as heterogeneous catalysis, material science, electrochemistry and corrosion. The bonding of molecular oxygen to metal atoms involving the formation of O_2^- ions is thus particularly important as it represents the initial stage of the long process that leads to the incorporation of oxygen into oxide lattices.

The superoxide anion has a $^2\Pi_g$ ground state and is readily detected by EPR spectroscopy when subjected to asymmetric electrostatic fields. In particular, the EPR technique has singularly advanced our understanding on the nature of the paramagnetic oxygen intermediates.[8,9]

The surface-adsorbed superoxide anion is usually identified on the basis of its g tensor, which is a very sensitive parameter of the electrostatic field of the adsorption site; however, only few examples are present in the literature in which the superhyperfine interaction with the adsorption site is detected.[9,10] Herein, we will show by means of hyperfine sublevel correlation (HYSCORE) spectroscopy that $Na^+O_2^-$ complexes are formed at the surface of MgO by interaction of gas-phase O_2 with deposited Na atoms. HYSCORE experiments allow the direct coordination of the O_2^- adsorbate to surface Na^+ cations to be proven, and in conjunction with DFT calculations, enable us to determine the structural details of the formed species.

Experimental and computational details

Experimental methods: High surface area (HSA) polycrystalline MgO was prepared by slow decomposition of the corresponding hydroxide in vacuum and was then activated at 1173 K to remove surface impurities. The surface area of the activated sample was about 200 $m^2 g^{-1}$. The sodium metal was distilled under vacuum to form a metal mirror in a separate part of the quartz cell used for the EPR measurements. The metal was evaporated on the sample in situ by heating the metallic mirror while keeping the powder at nearly room temperature.

---

[a] Dr. F. Napoli, Dr. M. Chiesa, Prof. E. Giamello
Dipartimento di Chimica IFM
Università di Torino and NIS
Nanostructured Interfaces and Surfaces Centre of Excellence
Via P. Giuria 7, I - 10125 Torino (Italy)
Fax: (+39)0116707855
E-mail: m.chiesa@unito.it

[b] Dr. G. Preda, Dr. C. Di Valentin, Prof. G. Pacchioni
Dipartimento di Scienza dei Materiali
Università di Milano-Bicocca
Via R. Cozzi, 53–20125, Milano (Italy)

CW and pulse EPR experiments were performed on an ELEXYS 580 Bruker spectrometer (microwave (mw) frequency 9.76 GHz) equipped with a liquid-helium cryostat from Oxford Inc. All experiments were performed at 10 K. The magnetic field was measured with a Bruker ER035M NMR Gaussmeter.

Electron-spin-echo (ESE) detected EPR experiments were carried out with the pulse sequence $\pi/2-\tau-\pi-\tau$-echo, with mw pulse lengths $t_{\pi/2}=16$ ns and $t_{\pi}=32$ ns, and a τ value of 200 ns. A repetition rate of 0.1 KHz was used. The EPR computer simulations were performed by using the EPRSIM32 program.

HYSCORE[11] experiments were carried out with the pulse sequence $\pi/2-\tau-\pi/2-t_1-\pi-t_2-\pi/2-\tau$-echo with mw pulse length $t_{\pi/2}=16$ ns and $t_{\pi}=16$ ns. The time intervals t_1 and t_2 were varied in steps of 16 ns starting from 96 ns to 2144 ns. Three different τ values were chosen ($\tau=104$, 124 and 256 ns). An eight-step phase cycle was used to eliminate unwanted echoes. The time traces of the HYSCORE spectra were baseline corrected with a third-order polynomial, apodized with a Hamming window and zero filled. After two-dimensional Fourier transformation, the absolute value spectra were calculated. The spectra were added for the different τ values to eliminate blind-spot effects. The HYSCORE spectra were simulated by using the Easyspin program.[12]

Computational methods: The properties of NaO_2 complexes formed at the MgO surface have been studied by means of embedded cluster models and DFT calculations using the B3LYP hybrid functional.[13,14] To properly account for the formation of strong dipoles on the surface resulting from the internal charge transfer in the $Na^+O_2^-$ units, the electronic relaxation of the substrate in a wide region was taken into account. This was based on the shell-model (SM) approach and the MgO surface was described by a nanocluster of about 5000 atoms. The central part, treated quantum-mechanically, is surrounded by a region of about 300 classical ions, the polarisability of which is described by a SM.[15] Cations in the SM region at the interface with the quantum mechanical (QM) region are replaced by ions (hereafter indicated as Mg*) on which a semi-local effective pseudopotential (ECP) is centred to reproduce the Pauli repulsion and avoid the non-physical polarisation of QM interface anions. Region I, which is made up of the QM and SM regions, is then surrounded by a large array of point charges (PC) to reproduce the long-range electrostatic potential.

This scheme is implemented in the GUESS code[16] interfaced with the Gaussian 03 code,[17] and the total energy of the hybrid system is calculated as a sum of classical and QM contributions. All centres in the QM region and Mg* interface atoms were allowed to move during the optimisation, whereas only shells, not cores, were relaxed in the SM region. In a few test cases the full relaxation, including the shells and cores, of the SM region have also been considered, but although the calculations are computationally much more expensive, the results are similar. Therefore, the electronic polarisation has been included in a large portion of the surface, although ionic polarisation is restricted to a few tens of atoms.

The following QM clusters have been considered to model edge, terrace, reverse-corner and reverse-edge sites: $Mg_{10}O_{10}Mg^*_{14}$ (edge), $Mg_{26}O_{14}Mg^*_4$ (terrace), $Mg_{17}O_{17}Mg^*_{22}$ (reverse corner), $Mg_{26}O_{26}Mg^*_{34}$ (reverse edge). The basis sets used were 6-31G on Mg, 6-31G* on the O atoms of MgO; for Na and the O_2 molecule the 6-311+G* basis set (geometry optimisation) and EPR-II basis set (computation of EPR parameters) were used, respectively.

The hyperfine interactions of the electron spin with the nuclear spin of the ^{23}Na and ^{17}O nuclides have been determined. The hyperfine spin Hamiltonian, $\mathscr{H}_{\rm hfc}=\mathbf{S}\cdot\mathbf{A}\cdot\mathbf{I}$, is given in terms of the hyperfine matrix **A**, which describes the coupling of the electron with the nuclear spin.[18] **A** can be represented as the sum of an isotropic ($a_{\rm iso}$) and a dipolar part **T** (**T** is a 3×3 traceless matrix).

To quantify the deviations of the g values of NaO_2 complexes from the free-electron value g_e, the spin–orbit interaction must be either accounted for self-consistently or be treated as a perturbation. Here we use the spin–orbit perturbation strategy in the scheme proposed by Neese[19] and implemented in the code Gaussian 03.[17]

Results and discussion

Continuous-wave EPR (CW-EPR) measurements: The interaction of alkali metal atoms with dehydrated HSA MgO leads to deeply blue coloured solids. Figure 1 a shows a representative X-band EPR spectrum at 77 K and low incident microwave power (0.1 mW) obtained by contacting a MgO sample with Na vapours. The spectrum is dominated by a quartet of lines characteristic of isolated monomeric species. The quartet of lines, with average separation of 14 mT, arises from the hyperfine interaction of the unpaired electron wave function with the sodium nucleus, $I=3/2$. The nature of this spectrum has been previously discussed by some of us,[2] and the reduction of the Na hyperfine constant of about 45 % with respect to the gas-phase value was demonstrated to be due to polarisation effects exerted by the surface binding site. Note that at approximately $g=2$ a signal is present in the experimental spectrum that includes contributions from small metal particles formed during the metal evaporation[20] and low-atomic-character species. The latter are always present upon interaction of alkali atoms with the surface and can be related to the presence of different surface point defects such as anion vacancies and residual surface OH^- groups. In particular, we demonstrated that residual hydroxyl groups present at the surface act as trapping sites for electrons originating from the ionisation of Na atoms and lead to the formation of so-called $(H^+)(e^-)$ paramagnetic centres, usually obtained by reaction of atomic hydrogen.[21] Further evidence for the presence of surface OH^- groups on the surface will be given below by means of HYSCORE spectroscopy.

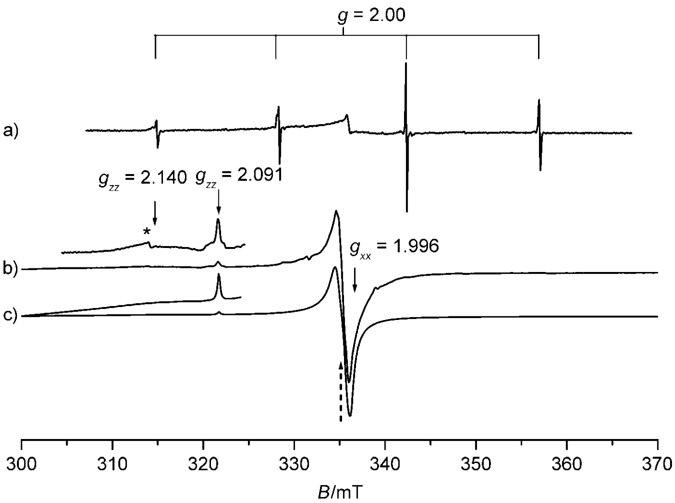

Figure 1. a) CW-EPR spectra of Na atoms deposited on the Na surface, b) Spectrum recorded upon reaction with 1.5 mbar of O_2, c) Computer simulation. All spectra were taken at 77 K. The asterisk indicates a Mn^{2+} impurity feature. The dashed arrow indicates the position where the HYSCORE spectrum reported in Figure 2 was taken.

Addition of 1.5 mbar of O_2 at room temperature lead to a bleaching of the sample and the quartet Na hyperfine pat-

Table 1. Spin Hamiltonian parameters of the various O_2^- species deduced from the simulation of CW-EPR and HYSCORE spectra. All hyperfine values are given in MHz.

Species	g_{xx}	g_{yy}	g_{zz}	^{23}Na				^{1}H			
				a_{iso}	T_{xx}	T_{yy}	T_{zz}	a_{iso}	T_{xx}	T_{yy}	T_{zz}
O_2^-/HMgO	2.008	2.002	2.0910 ± 0.002	–	–	–	–	-5.0 ± 0.5	-9.8 ± 0.1	$+19.6\pm0.1$	-9.8 ± 0.1
O_2^-/NaMgO	2.008	2.002	2.14 ± 0.04	-15.0 ± 2	-0.1 ± 0.5	$+3.1\pm0.5$	-3.0 ± 0.5	–	–	–	–
NaO_2[a]	2.0075	2.0022	2.1106	-9.1	-1.5	$+3.0$	-1.5	–	–	–	–

[a] Data taken from Ref. [26].

tern spectrum was replaced by a new signal shown in Figure 1b. This new spectrum was characterised by an orthorhombic powder pattern, characteristic of surface-adsorbed superoxide O_2^- species. More detailed analysis of the spectrum by using computer simulation (Figure 1c) indicates that several species contribute to the spectrum, which can be interpreted as the superposition of different O_2^- ions adsorbed on various surface sites, mainly characterised by different g_{zz} factors (Table 1). The **g** matrix is typical for a bound $^2\Pi_{3/2}$ state in which the local C_{2v} crystal field gives rise to an orthorhombic g tensor with $g_{zz} \gg g_{yy} > g_{xx} \approx g_e$ (in which the z direction lies along the internuclear O_2^- axis, whereas the x direction coincides with the cation–superoxide bond axis), given by classic expressions[22] characterised by the unpaired electron on the out-of-plane $|\pi^*(2p_y)\rangle$ antibonding orbital, which can be described by Equations (1)–(3) in which λ is the spin-orbit coupling constant, Δ is the $2p\pi_g^{\,y}$–$2p\pi_g^{\,x}$ separation and E is the $2p\pi_g^{\,y}$–$2p\sigma_g$ separation. It then follows that $g_{zz} \gg g_{yy} > g_{xx}$ in agreement with the experimentally observed values.

$$g_{xx} = 2.0023[\Delta^2/(\lambda^2+\Delta^2]^{1/2} - \lambda/E\{[\lambda^2/(\lambda^2+\Delta^2)]^{1/2} - [\Delta^2/(\lambda^2+\Delta^2]^{1/2} - 1\} \tag{1}$$

$$g_{yy} = 2.0023[\Delta^2/(\lambda^2+\Delta^2]^{1/2} - \lambda/E\{1 - [\lambda^2/(\lambda^2+\Delta^2)]^{1/2} - [\Delta^2/(\lambda^2+\Delta^2]^{1/2}\} \tag{2}$$

$$g_{zz} = 2.0023 + 2[\lambda^2/(\lambda^2+\Delta^2]^{1/2} \tag{3}$$

The energy splitting between the π^* orbitals (Δ), is caused by the surface crystal field, which in turn directly depends on the charge of the cation onto which O_2^- is adsorbed. The g_{zz} component can thus be used to determine the nature of the adsorption site in cases in which more than one type of cation is present, such as in this case.

The low-field region (g_{zz}) of the spectrum is characterised by a sharp feature at $g_{zz}=2.091$, which is easily assigned to classic superoxide ions on Mg^{2+}.[23] In particular, the $g_{zz}=2.091$ component of O_2^- adsorbed on MgO has been assigned by some of us[24,25] to radicals stabilised by five-coordinated cations at MgO (100) terraces and formed upon direct electron transfer from molecular adsorbates.

Together with this feature a very-broad band is observed in the experimental spectrum centred at lower field values at about $g_{zz}=2.14$. Such a g value is typical of superoxide anions stabilised on monovalent cations and is in line with g values observed for matrix-isolated alkali metal superoxides[26] and O_2^- adsorbed on Cs^+ ions stabilised at the surface of MgO.[10] The broad linewidth that characterises the spectrum is indicative of a relatively large distribution of values (strains) due to slightly different local environments probed by the adsorbed superoxide on different surface sites. This effect, also referred to as speciation, is often encountered in the case of paramagnetic species stabilised on polycrystalline surfaces. Together with g strain effects, unresolved hyperfine interactions arising from a small delocalisation of the unpaired electron spin density on Na nuclei will also contribute to broaden the spectral linewidth, indicating that the superoxide species characterised by the broad $g_{zz}=2.14$ component can be assigned to a surface O_2^-–Na^+ adduct. The small hyperfine interactions hidden by the inhomogeneous line broadening can be resolved by means of ESEEM (electron-spin-echo envelope modulation) experiments. In particular HYSCORE experiments allowed the full ^{23}Na hyperfine coupling tensor to be determined.

HYSCORE experiments: HYSCORE is a two-dimensional ESEEM spectroscopic technique in which a mixing π pulse creates correlation of nuclear frequencies in one electron spin (m_S) manifold to nuclear frequencies in the other manifold, allowing weak hyperfine and nuclear quadrupole couplings to unravel.

The HYSCORE spectrum taken at observer position $B_0=346.3$ mT (corresponding to the dashed arrow in Figure 1b) is reported in Figure 2a. This magnetic field setting corresponds to the g_x/g_y position of the superoxide anion. Similar spectra were obtained at field positions spanning the g_x/g_y spectral region (i.e., 330–340 mT in Figure 1b). The spectrum contains three sets of cross-peaks resulting from interactions with distinct ^{23}Na and ^{1}H nuclei. Two off-diagonal cross-peaks are present in the (-,+) quadrant at (−11.6, 4.2) MHz and (4.2, −11.6) MHz. As expected in the case of a strong hyperfine coupling ($|A|>2\nu_I$), the cross-peaks are separated by approximately 2 ν_{Na} ($\nu_{Na}=3.944$ MHz). The two peaks (labelled ^{23}Na(I) in Figure 2a) cross the antidiagonal at about 8.5 MHz, indicating a maximum hyperfine coupling of about 17 MHz. Two distinct signals are then observed in the (+,+) quadrant centred at the ^{1}H and the ^{23}Na nuclear Zeeman frequency. The pronounced ridge, centred at about (15, 15) MHz (close to the ^{1}H nuclear Zeeman frequency, $\nu_H=14.9021$ MHz) with a width of about 14 MHz is due to the ^{1}H superhyperfine interaction with residual OH^- groups present at the surface of MgO, whereas the signal centred at the ^{23}Na nuclear Zeeman frequency with

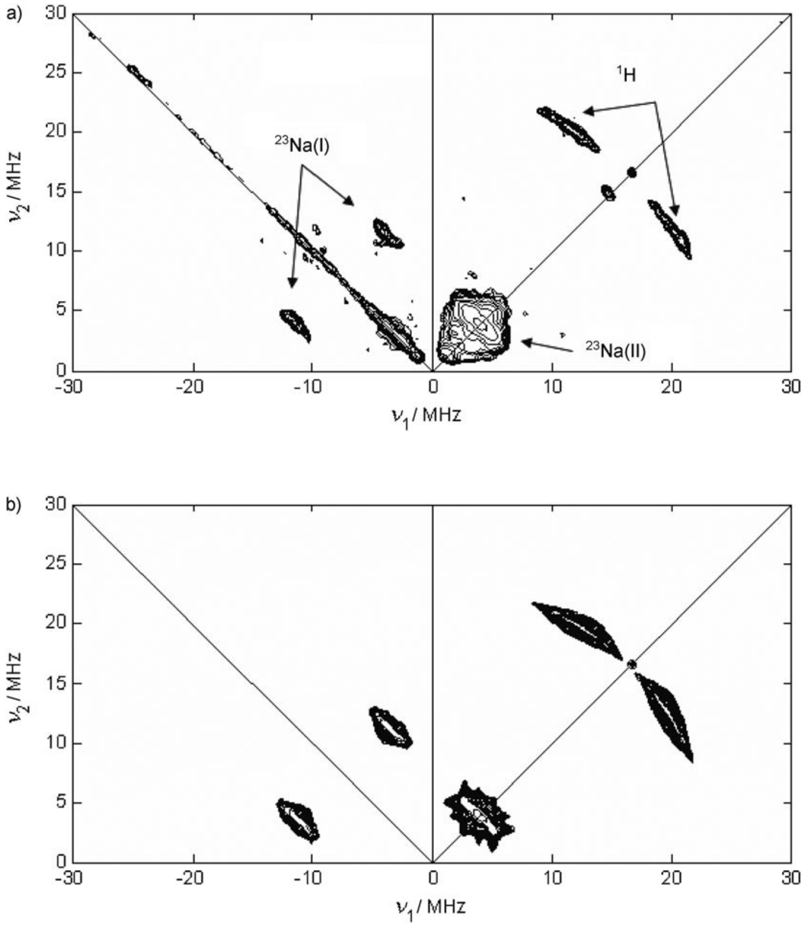

Figure 2. a) Experimental and b) simulated HYSCORE spectra of O_2^- species on Na/MgO. The spectra were recorded at 10 K.

maximum extension of about 3.0 MHz (labelled ^{23}Na(II) in Figure 2a) stems from the interaction of the superoxide with a second set of weakly interacting sodium nuclei.

Computer simulation of the spectrum (Figure 2b) was performed to extract the spin Hamiltonian parameters for the ^{23}Na and ^{1}H superhyperfine interaction (Table 1). The nuclear quadrupole couplings for the ^{23}Na case were found to be small ($e^2qQ/h \cong 1$ MHz), consistent with the narrow form of the single quantum cross-peaks and the lack of multiple quantum features in the HYSCORE spectra. The values fall within the typical range reported for this nucleus.[27,28] The absence of combination peaks appears to indicate that these interactions result from different superoxide species localised at different surface sites (speciation). This is consistent with the two different g_{zz} factors (2.14 and 2.091) observed in the CW-EPR spectrum.

Full evaluation of the ^{23}Na tensor requires HYSCORE spectra to be measured in correspondence with the g_{zz} component. Owing to the low spectral intensity at this field position, however, the ^{23}Na signal is barely detectable. Simulation analysis of the ^{23}Na HYSCORE spectrum, however, allows the fact that the interaction is characterised by a large Fermi contact term to be firmly established. Moreover, considering the Na–O_2 interatomic distance in molecular sodium superoxide deduced from vibrational spectra (1.96 Å),[29] and by assuming an ionic model, the largest dipolar coupling (T_y) can be evaluated to be of the order of 3 MHz.[26] Based on these considerations and on the simulation analysis of the spectrum we find $a_{iso} = (-15 \pm 2)$ MHz and an anisotropic **T** tensor $((-3.0 \pm 0.5)\ (-0.1 \pm 0.5)\ (+3.1 \pm 0.5))$ MHz, in which a negative value was assigned to a_{iso} to allow for a positive anisotropic hyperfine component T_z. This analysis is supported by DFT calculations (see below). These values, and in particular the high a_{iso} value, indicate a considerable degree of interaction thus providing evidence for a direct bonding of the superoxide molecular anion to surface Na^+ species. From the value of the dipolar interaction the Na^+–O_2^- distance can be estimated, which is of the order of 2 Å. The observed results are in line with those reported for NaO_2 molecular species trapped in rare-gas matrixes.[26] Interestingly, the degree of interaction in the case of the surface adducts appears to be more pronounced. This same effect was also observed in the case of O_2^- species bound to Cs^+ cations on the surface of MgO.[10] This aspect will be further explored by means of quantum chemical calculations.

The weakly ^{23}Na-coupled signal observed in the (+,+) quadrant was simulated by considering the contribution of non-nearest ^{23}Na nuclei. In an oversimplified scheme, by considering the O_2^- adsorbed on a five-fold coordinated Mg^{2+} cation (Mg–O distance = 2.05 Å), non-nearest Na nuclei are found in every model to be at distances of at least about 4 Å. This means that the anisotropic part will be $(-0.35\ -0.35\ +0.7)$ MHz or less. The analysis shows that the width of the ridge can be reproduced if a distribution of ^{23}Na in the range between 3.5 Å and 4.5 Å is considered, corresponding to $-0.2 < T -0.5$ MHz. In Figure 2b the simulation obtained with $A = (-3\ -3\ -1.5)$ MHz, $|e^2qQ/h| = 1$ MHz, $\eta = 0$ is reported (η = asymmetry parameter). This is consistent with the lack of multiple quantum features, which typically appears in the case of $S = 1/2$ $I = 3/2$ systems for $T_\perp > 1$ MHz and higher quadrupolar couplings.[30] Therefore, it appears to be realistic to assign the ^{23}Na(II) signal to the superhyperfine interaction of O_2^- ions with non-nearest Na^+

ions. Both superoxide families characterised by $g_{zz}=2.091$ and $g_{zz}=2.14$ can be associated to this weak interaction.

Finally, the pronounced broad proton ridge with maximum extension of about 15.7 MHz reveals the interaction of O_2^- species to a nearby proton. The presence of surface hydroxyl protons was anticipated above based on a signal at $g=2.00$, which is characteristic of $(H^+)(e^-)$ surface centres. These centres readily react with molecular oxygen to form O_2^- radicals, characterised by a residual superhyperfine interaction with a nearby proton.[31] This interaction is clearly revealed by the proton ridge observed in the (+,+) quadrant of the HYSCORE spectrum. By assuming an axially symmetric proton hyperfine interaction tensor, ${}^{H}T_{\perp}=$ 9.8 MHz can be estimated from the maximum shift $\Delta\nu(H)_{max}{}^{s}=1.86$ MHz of the proton ridge.[32] This value is in good agreement with that reported by Diwald and Knözinger[33] for O_2^- species, characterised by the same g_{zz} value, obtained by intermolecular electron transfer of pre-adsorbed H_2 towards O_2. Computer simulation of the spectrum allows an a_{iso} of the order of -5 MHz to be determined. The angle β between the g_{zz} and the ${}^{H}A_{zz}$ axes is found to be in the range 45–90°. A more detailed analysis of the $O_2^-- H^+$ interaction will be the object of a forthcoming study. Owing to the low spectral resolution at field positions corresponding to the g_{zz} spectral components, it was not possible to reliably obtain the Euler angles relating the ^{23}Na and ^{1}H hyperfine tensors.

Based on the above reported experimental results we can propose a general model for the reaction of O_2 with Na adsorbed atoms on MgO. The result of Na evaporation on MgO is schematically resumed in Scheme 1 a, in which the three main paramagnetic species detected by CW-EPR, namely, Na adsorbed atoms, $(H^+)(e^-)$ centres and small sodium metal particles are indicated. Superoxide ions are formed by electron transfer at the expense of the above-mentioned species. A fraction of the radical ions are stabilised on the resulting Na^+ cations (labelled as 1 in Scheme 1 b) leading to EPR spectra characterised by high g_{zz} factors and relatively large ^{23}Na hyperfine interactions. A second family of O_2^- radicals is stabilised on Mg^{2+} matrix sites in the proximity of a surface OH^- group (labelled as 2 in Scheme 1 b). This second family can arise by direct electron transfer from surface $(H^+)(e^-)$ centres or through a spill-over mechanism involving small metal particles. Below we will concentrate on the first family of superoxide anion radicals with the aim to provide, by means of DFT calculations, a tentative structural assignment for the NaO_2/MgO complexes described above.

DFT calculations: DFT calculations have been carried out on various models. In particular, we have considered three systems to assess the quality of the computational results and to provide a solid basis for the assignment. Besides various types of NaO_2 complexes formed at different sites of the MgO surface (Figure 3 and Table 2), we have considered the free, gas-phase NaO_2 molecule as well as the properties of O_2^- superoxo species formed at the MgO surface. For each species the **g** matrix and the hyperfine coupling constants (both isotropic and dipolar parts) with ^{23}Na and ^{17}O have been calculated and compared with available experimental data. We started our analysis from the free NaO_2 molecule, keeping in mind that the experiments refer to species isolated in rare-gas matrices.[26] The experimental **g** tensor is characterised by one component, $g_{xx}=2.002$, very close to the free-electron value, a second component that is only moderately shifted, $g_{yy}=2.006$, and a g_{zz} term at 2.110 that exhibits a large shift from the free-electron value (the same reference axis system described above in Equations (1)–(3) is adopted).[26] The calculations reproduce this structure, with the three components of the **g** tensor at 2.0023, 2.0098 and 2.0740 (Table 2). However, in absolute terms the g_{zz} component is underestimated by $\Delta g=0.036$. This difference, which is also found for other oxygen species, must be taken into account when we compare the results for more complex systems. The structure of the ^{23}Na hyperfine coupling constant is reproduced with good accuracy. In particular, the dominant a_{iso} term is well described in the calculations (Table 2) and, in general, the absolute error is of the order of 2 MHz.

As a second term of comparison we considered O_2^- superoxo ions stabilised on the edge and terrace sites of the clean MgO surface (Figure 3 a and b). In the experiment, the structure of the **g** matrix is similar to that in NaO_2 with a small g_{yy} component that is slightly reduced compared with g_e, one component, g_{xx}, which is slightly increased, and a third term that is considerably shifted to higher values. This last term is particularly important because, as discussed in the previous section, it is very sensitive to the site or to the charge of the cation where O_2^- is adsorbed. Typical experimental g_{zz} values for O_2^- adsorbed on MgO are 2.077 and 2.091,[34] and have been assigned to O_2^- adsorbed on edge

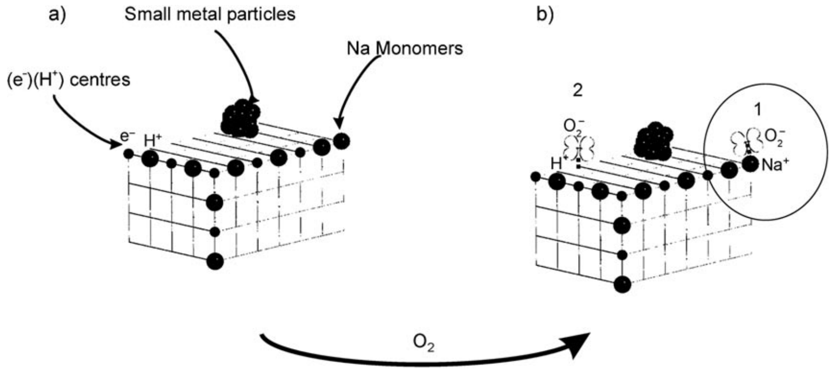

Scheme 1. Schematic representation of a) paramagnetic species formed upon sodium evaporation on MgO and b) the two main families of O_2^- formed upon reaction of O_2. The dominant species discussed in the text are highlighted in the circle.

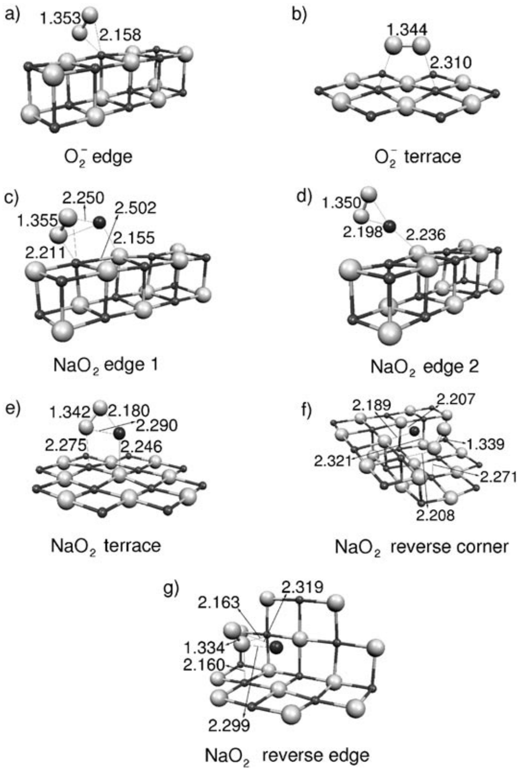

Figure 3. a) and b) O_2^- species formed at edge and terrace sites, respectively, of the MgO surface. NaO_2 species formed at c) edge 1, d) edge 2, e) terrace, f) reverse-corner, g) reverse-edge sites of the MgO surface (white spheres: O, grey spheres: Mg, black spheres: Na).

or terrace sites, respectively.[24,25,35] Note that both of these values are smaller than the g_{zz} component in NaO_2 (2.110). In the present calculations, O_2^- adsorbed on an edge or a terrace site of MgO is characterised by $g_{zz}=2.0525$ and $g_{zz}=2.0639$, respectively (Table 2). As for the NaO_2 case, the absolute values are underestimated compared with the experiment. However, the difference between the edge and terrace, $\Delta g=0.011$, is similar to that found in the experiment, $\Delta g=0.014$. Even more important, the g_{zz} values for O_2^-/MgO are smaller than those computed for NaO_2, in line with the experiment. The hyperfine constants for ^{17}O in O_2^-/MgO are known experimentally (Table 2). The calculations show that this property is not very dependent on the adsorption site, being essentially related to the spin distribution in the O_2^- unit. Although the dipolar part of the tensor is reproduced quantitatively, with errors of less than 2%, the isotropic part is reproduced only qualitatively, with an error of about 30% (Table 2). This is a well-known fact, in particular for oxygen-containing molecules, and has been discussed in detail in the literature.[36] Thus, we can conclude that, in general, the calculations provide a satisfactory description of the known systems containing the superoxo species, the NaO_2 molecular unit on one side and the O_2^-/MgO surface complexes on the other. The comparison with experiment also provides a benchmark of the accuracy of the calculations. With this information we can now consider explicitly models of NaO_2 complexes formed at the MgO surface.

We have studied a large number of possible structures formed at various sites. For reasons of brevity, we will only discuss here those structures that are relevant in terms of stability or of consistency with the experimental data. A first consideration is related to the fact that the experiment is performed by dosing O_2 on a Na pre-covered MgO surface. In an initial stage, therefore, it can be reasonably assumed that the NaO_2 complexes will form at the surface sites where Na atoms are preferentially stabilised. This

Table 2. Computed EPR parameters for O_2^- and NaO_2 complexes formed at the surface of MgO (hyperfine coupling constants are in MHz). E=edge, T=terrace, RC=reverse corner, RE=reverse edge.[a]

				^{17}O (MHz)				^{23}Na (MHz)			
	g_{xx}	g_{yy}	g_{zz}	a_{iso}	T_{xx}	T_{yy}	T_{zz}	a_{iso}	T_{xx}	T_{yy}	T_{zz}
Experiment											
NaO_2[b]	2.0075	2.0022	2.1106	–	–	–	–	−9.1	−1.5	+3.0	−1.5
O_2^-/MgO E[c]	2.0083	2.0016	2.0770	−56.5	+76.7	−157	+80.6	–	–	–	–
O_2^-/MgO T[d]	2.008	2.002	2.0910	–	–	–	–	–	–	–	–
NaO_2/MgO	2.00	2.00	2.14	–	–	–	–	−15.0	−0.1	+3.1	−3.0
Theory											
NaO_2[e]	2.0098	2.0023	2.0740	−29.7	82.3	−168.7	86.4	−11.5	−1.8	3.7	−1.9
O_2^-/MgO E (Figure 3a) [f,g]	2.0096	2.0021	2.0527	−37.9	80.2	−163.4	83.2	–	–	–	–
O_2^-/MgO T[f,g] (Figure 3b)	2.0092	2.0022	2.0639	−39.2	78.7	−160.3	81.8	–	–	–	–
NaO_2/MgO E1 (Figure 3c)[g]	2.0104	2.0021	2.0893	−39.0	79.4	−161.5	82.1	−20.0	−0.3	3.5	−3.2
NaO_2/MgO E2[e] (Figure 3d)	2.0094	2.0021	2.0721	−38.1	79.6	−163.4	83.5	−8.7	−1.7	3.4	−1.7
NaO_2/MgO T[e,h] (Figure 3e)	2.0092	2.0021	2.0866	−37.2	74.2	−151.6	77.4	−10.7	−0.8	2.7	−1.9
				−37.9	83.7	−171.0	87.4				
NaO_2/MgO RC[g,h] (Figure 3f)	2.0094	2.0021	2.1030	−38.6	69.5	−141.8	72.2	−13.9	−0.2	2.2	−2.0
				−39.8	87.5	−177.6	90.1				
NaO_2/MgO RE[g,h] (Figure 3g)	2.0096	2.0021	2.1650	−41.7	72.2	−146.7	74.4	−15.0	−0.4	3.0	−2.6
				−40.2	83.8	−170.7	86.9				

[a] The reference coordinate system for the **g** and **T** tensors: The z axis is the internuclear O–O axis, the xz plane is the M(O–O) plane, the y axis is perpendicular to the xz plane. The unpaired electron is in the π^*_y orbital. In the cases in which two interacting M atoms exist (Na or a surface Mg) the relevant M is specified. [b] From Ref. [26]. [c] From Ref. [34]. [d] From Ref. [35]. [e] The relevant M is Na in this case. [f] The calculations have been performed without inclusion of the long-range polarisation (shell model). [g] The relevant M is Mg in this case. [h] The two O atoms of the O_2^- molecule are non-equivalent. The first line refers to the O atom at direct contact with the MgO surface.

aspect has been investigated in detail in the past.[3] Although a definitive conclusion on the preferred adsorption sites is not possible given the existence of a few isoenergetic positions, there is evidence that among the most likely adsorption sites for Na are the edges, the reverse corners and the reverse edges, which, given the computed stability, can be populated at room temperature. The corresponding stabilities of the Na atoms are 0.69 (edge), 0.59 (reverse edge), 0.79 (cationic reverse corner) and 1.49 eV (anionic reverse corner).[3] For this reason we start the discussion from NaO_2 formed on an edge site (Figure 3c). The Na atom is interacting with an O ion of the surface at a distance of about 2.2 Å. In this position the 3s valence electron is still associated to the Na atom (the atom is neutral), but is strongly polarised.[3] The O_2 molecule has been placed at bonding distances from this atom and the geometry optimisation started from various orientations (monodentate, bidentate, parallel, linear, bent). In all cases a net charge transfer occurs spontaneously with formation of a $Na^+O_2^-$ complex. The energy gain is rather large, 2.31 eV in the most stable structure (Figure 3c and Table 3). Here the O_2 molecule is interacting simultaneously with the Na^+ cation and with a four-coordinated Mg^{2+} cation of the edge; in this way, the O_2^- unit benefits from the electrostatic interaction with two cations. The O—O bond is perpendicular to the edge, the two O atoms are equivalent and the unpaired electron is localised in a π* orbital lying in the Na(O—O) plane. In the next stable isomer the O_2 molecule is bound to Na but not to the surface (Figure 3d). This structure is 0.4 eV less stable than the ground-state isomer (Table 3). In this second structure the O_2 molecule is free to rotate around the O—Na axis (the barrier for rotation is only 0.01 eV) and the π* orbital hosting the unpaired electron is found to be perpendicular to the Na(O—O) plane as in the case of the NaO_2 free molecule.

Table 3. Adsorption energy, E_a, of O_2 molecules on Na/MgO and of NaO_2 molecules on MgO.

NaO_2/MgO adsorption site	E_a (O_2) [eV][a]	E_a (NaO_2) [eV][b]
edge 1 (Figure 3c)	2.31	3.01
edge 2 (Figure 3d)	1.92	2.62
terrace (Figure 3e)	2.19	1.12
reverse corner (Figure 3f)	3.01	2.69
reverse edge (Figure 3g)	2.74	3.53

[a] Defined as E_a (O_2) = [E(NaO_2/MgO)−E(Na/MgO)−E(O_2)]. [b] Defined as E_a (NaO_2) = [E(NaO_2/MgO)−E(MgO)−E(NaO_2)].

We consider now the EPR properties of the most stable of the two isomers (Figure 3c and Table 2). The **g** tensor has the same structure already found for gas-phase NaO_2, with one term close to g_e, $g_{yy} = 2.0021$, a component slightly shifted, $g_{xx} = 2.0104$, and a third component that deviates strongly from g_e, $g_{zz} = 2.0893$. This latter term, in the calculations, is larger than the corresponding theoretical value of free NaO_2, $g_{zz} = 2.0740$, in full agreement with the experiment in which g_{zz}(NaO_2/MgO) is larger than g_{zz}(NaO_2). This is an important result because it demonstrates that the purely ionic model in which the g_{zz} factor is determined by the local crystal field of the adsorbing ion (Equation (3)) has to be handled with care. Based on these arguments, the case represented in Figure 3c would be expected to have a g_{zz} factor smaller than the case of Figure 3d, the fist case being the O_2^- adsorbed on a Mg^{2+} ion and the second case being on a Na^+ ion . The calculations show that this trend is reversed, indicating a non-negligible role of covalency in the NaO_2/MgO system. Of course, the absolute values differ significantly, the calculated g_{zz} for NaO_2/MgO (edge 1) being $g_{zz} = 2.0893$, which is much smaller than in the experiment ($g_{zz} \cong 2.14$, Table 2). However, we have seen above that this is a general systematic error. Therefore, we can conclude that the **g** matrix for a NaO_2 complex formed on an edge site of MgO is consistent with the experimental data.

Further support to this assignment comes from the analysis of the ^{23}Na hyperfine coupling constants. These are reproduced in an almost quantitative way for free NaO_2 (Table 2). On the NaO_2/MgO (edge 1) species, a_{iso} is −20.0 MHz compared with $a_{iso} = -11.5$ MHz in NaO_2, which has increased by about 70%; the dipolar part remains small and almost unchanged. In the experiment, going from matrix-isolated NaO_2 to MgO supported NaO_2 a_{iso} goes from −8.9 to −15.6 MHz with the same relative increase of the computational model. In this case, the absolute values of the hyperfine constants are also reproduced with acceptable errors and, in particular, the departure from axial symmetry of the **T** tensor is correctly reproduced. Notice that if we consider the second stable isomer (Figure 3d) the agreement with experiment is much less satisfactory. First the g_{zz} value is nearly the same as in free NaO_2 and not larger, at variance with the experiment (Table 2). Second, a_{iso}(^{23}Na) is smaller than in free NaO_2 and not larger, and the **T** tensor displays axial symmetry, again in contradiction with the observations. This shows that the structure of the EPR spectrum is very sensitive to the exact orientation of the NaO_2 surface complex and that the isomer shown in Figure 3d is inconsistent both in terms of stability and of EPR properties. Similar complexes, in which O_2 interacts only with Na and not with the MgO surface (see Figure 3d) but is formed at other sites like terraces or corners, exhibit the same inconsistency, so that in the assignment one can rule out these structures.

As mentioned above, the computed hyperfine coupling constants (HFCCs) for ^{17}O in superoxo O_2^-/MgO species are not very informative about the nature of the adsorption site because they do not change substantially from site to site (Table 2). However, the hyperfine tensor orientation provides a clear indication of the π* orbital hosting the unpaired electron. In some cases (Figure 3d and e, discussed below) the electron is in the π* orbital perpendicular to the Na(O—O) plane, in other cases (Figure 3c, f and g, discussed below) it is in the π* orbital perpendicular to the Mg_s(O—O) plane, in which Mg_s is the surface Mg ion interacting with the O_2^- species. These latter models are consistent with the experimental observation in terms of both EPR properties (**g** and **A** tensors) and energetic properties.

Based on the analysis of the full set of EPR parameters, **g** and **A** tensors, the NaO_2 species formed on an edge site of the MgO surface where O_2 is simultaneously bound to Na and to MgO, Figure 3c, epitomises the structural characteristics of the species responsible for the large g shift and ^{23}Na hyperfine interaction observed in the EPR experiments.

In the rest of the discussion we will briefly present a few selected results for three other sites. As a first case we consider a NaO_2 complex formed at the MgO(100) terrace (Figure 3e). Note that because Na atoms are not stabilised at these sites,[3] this situation can be found only by assuming a diffusion process for the NaO_2 units. In the most stable isomer the O_2^- superoxide anion interacts with the Na atom and with a surface Mg^{2+} cation with a binding energy of 2.19 eV, Table 3, similar to the edge case. Overall, however, the NaO_2 unit is much more stable on the edge, where it is bound by 3.01 eV, whereas on the terrace the bonding is only 1.12 eV (Table 3). In this configuration (Figure 3e) the **g** tensor is consistent with the experiment ($g_{zz}(NaO_2/MgO) > g_{zz}(NaO_2)$, Table 2) but the **A** tensor is not (a_{iso} is smaller than in free NaO_2, whereas in the experiment it is larger). So, not only is the terrace complex (Figure 3e) thermodynamically less favourable than the edge one, but its EPR parameters do not fit with the observation.

Much more interesting from this point of view are the other two cases considered, namely, a Na atom stabilised at reverse-corner and reverse-edge sites, two of the most strongly binding sites on the MgO surface. On the reverse corner, the Na atom interacts with three oxide anions and binds O_2 by 3.01 eV (Table 3). The O_2 molecule interacts with both Na and Mg^{2+} cations of the step (Figure 3f) but owing to the local conformation, the two oxygen atoms are non-equivalent. The NaO_2 unit is bound to this site by 2.69 eV, that is, slightly less than on an edge site (Table 3). The **g** tensor exhibits, among the cases considered, the best agreement with the experiment. In fact, the g_{zz} component 2.1030 is 0.029 higher than in free NaO_2 ($g_{zz}=2.0740$); in the experiment the difference is 0.028 (see Table 2). The a_{iso}(^{23}Na) value, −13.9 MHz, is also higher than in the free molecule, −11.5 MHz, although here the relative change (+20%) is smaller than the measured one (+75%). On the reverse edge (Figure 3g) the Na atom is bound to two O ions of the surface and the NaO_2 unit has similar characteristics to those for the other irregular sites, that is, it is strongly bound, (3.53 eV, Table 3), and the two O atoms of the O_2^- molecule are no longer equivalent. In this conformation, the O_2^- molecule exhibits the highest g_{zz} value computed so far, 2.1650, which is even higher than in NaO_2 (Table 2). The coupling with ^{23}Na is similar to that computed for the edge and reverse-corner cases (Table 2).

In summary, the NaO_2 complexes formed at reverse-corner and reverse-edge sites are also compatible with the experimental data, and it is likely that a family of sites is populated. This is in line with the broad g_{zz} feature centred at about 2.14 observed in the experimental CW-EPR spectrum, which can indeed be explained by taking into account a distribution of slightly different surface adsorption sites.

Conclusion

In a combined EPR (CW-EPR and HYSCORE) and DFT study, the reactivity of O_2 with Na atoms adsorbed on the surface of polycrystalline MgO has been investigated. Direct surface to adsorbate electron transfer has been observed leading to O_2^- radical anions stabilised at different surface sites. HYSCORE measurements allowed the investigation of the ligand hyperfine coupling between O_2^- electron spin and ^{23}Na and ^{1}H nuclei present at the MgO surface, proving that a fraction of the formed superoxide is indeed chemically bound to the surface Na^+ ions, while a second fraction is stabilised on the MgO matrix. Comparison with rare-gas matrix-trapped NaO_2 molecules shows that the MgO stabilised complex is characterised by larger a_{iso} and g_{zz} parameters. The differences between isolated molecular species and surface-adsorbed species have been rationalised with the help of DFT calculations. These lend support to the analysis of the HYSCORE data allowing the clarification of the structural and electronic characteristics of the NaO_2/MgO complex. In particular, the calculations show that the role of the matrix is instrumental in stabilising the so-formed superoxide, leading to a counterintuitive positive shift of the g_{zz} component. A family of sites are found to be compatible with the observed experimental results, which are characterised by a mutual interaction of the superoxide radical anion with Mg^{2+} matrix ions and surface Na^+ species. Interestingly, in the case of the surface-stabilised NaO_2 complex the unpaired electron is found to be located in a π^* orbital dwelling in the O_2–Na plane, whereas the reverse occurs for matrix trapped NaO_2 molecules.

Finally, it can be concluded that HYSCORE spectroscopy in conjunction with DFT modelling is a powerful tool to explore the structure of paramagnetic species localised at solid surfaces, allowing specific binding sites and geometrical and electronic structures of surface-adsorbed species to be established.

Acknowledgements

We thank the support from the COST Action D41.

[1] M. Chiesa, E. Giamello, C. Di Valentin, G. Pacchioni, Z. Sojka, S. Van Doorslaer, *J. Am. Chem. Soc.* **2005**, *127*, 16935.
[2] M. Chiesa, F. Napoli, E. Giamello, *J. Phys. Chem. C* **2007**, *111*, 5481.
[3] E. Finazzi, C. Di Valentin, G. Pacchioni, M. Chiesa, E. Giamello, H. J. Gao, J. C. Lian, T. Risse, H-J. Freund, *Chem. Eur. J.* **2008**, *14*, 4404.
[4] G. Preda, G. Pacchioni, M. Chiesa, E. Giamello, *Phys. Chem. Chem. Phys.* **2009**, *11*, 8156.
[5] M. Anpo, M. Che, B. Fubini, E. Garrone, E. Giamello, M. C. Paganini, *Top. Catal.* **1999**, *8*, 189.
[6] R. Davydov, J. D. Satterlee, H. Fujii, A. Sauer-Masarwa, D. H. Busch, B. M. Hoffman, *J. Am. Chem. Soc.* **2003**, *125*, 16340.
[7] G. Henrici-Olivè, S. Olivè, *Angew. Chem.* **1974**, *86*, 1; *Angew. Chem. Int. Ed. Engl.* **1974**, *13*, 29.
[8] Z. Sojka, *Cat. Rev. Sci. Eng.* **1995**, *37*, 461.
[9] M. Che, A. J. Tench, *Adv. Catal.* **1982**, *31*, 77.

[10] M. Chiesa, M. C. Paganini, E. Giamello, D. M. Murphy, *J. Phys. Chem. B* **2001**, *105*, 10457.
[11] P. Höfer, A. Grupp, H. Nebenfür, M. Mehring, *Chem. Phys. Lett.* **1986**, *132*, 279.
[12] S. Stoll, A. Schweiger, *J. Magn. Reson.* **2006**, *178*, 42.
[13] A. D. Becke, *J. Chem. Phys.* **1993**, *98*, 5548.
[14] C. Lee, W. Yang, R. G. Parr, *Phys. Rev. B* **1988**, *37*, 785.
[15] B. G. Dick, A. W. Overhauser, *Phys. Rev.* **1958**, *112*, 90.
[16] P. V. Sushko, A. L. Shluger, C. R. A. Catlow, *Surf. Sci.* **2000**, *450*, 153.
[17] Gaussian 03, Revision A.7, M. J. Frisch, G. W. Trucks, H. B. Schlegel, G. E. Scuseria, M. A. Robb, J. R. Cheeseman, J. A. Montgomery, Jr., T. Vreven, K. N. Kudin, J. C. Burant, J. M. Millam, S. S. Iyengar, J. Tomasi, V. Barone, B. Mennucci, M. Cossi, G. Scalmani, N. Rega, G. A. Petersson, H. Nakatsuji, M. Hada, M. Ehara, K. Toyota, R. Fukuda, J. Hasegawa, M. Ishida, T. Nakajima, Y. Honda, O. Kitao, H. Nakai, M. Klene, X. Li, J. E. Knox, H. P. Hratchian, J. B. Cross, V. Bakken, C. Adamo, J. Jaramillo, R. Gomperts, R. E. Stratmann, O. Yazyev, A. J. Austin, R. Cammi, C. Pomelli, J. W. Ochterski, P. Y. Ayala, K. Morokuma, G. A. Voth, P. Salvador, J. J. Dannenberg, V. G. Zakrzewski, S. Dapprich, A. D. Daniels, M. C. Strain, O. Farkas, D. K. Malick, A. D. Rabuck, K. Raghavachari, J. B. Foresman, J. V. Ortiz, Q. Cui, A. G. Baboul, S. Clifford, J. Cioslowski, B. B. Stefanov, G. Liu, A. Liashenko, P. Piskorz, I. Komaromi, R. L. Martin, D. J. Fox, T. Keith, M. A. Al-Laham, C. Y. Peng, A. Nanayakkara, M. Challacombe, P. M. W. Gill, B. Johnson, W. Chen, M. W. Wong, C. Gonzalez, J. A. Pople, Gaussian, Inc., Wallingford CT, **2003**.
[18] *Electron Paramagnetic Resonance* (Eds.: M. Brustolon, E. Giamello), Wiley, New York, **2009**.
[19] F. Neese, *J. Chem. Phys.* **2001**, *115*, 11080.
[20] D. M. Murphy, E. Giamello, *J. Phys. Chem.* **1994**, *98*, 7929.
[21] F. Napoli, M. Chiesa, E. Giamello, E. Finazzi, C. Di Valentin, G. Pacchioni, *J. Am. Chem. Soc.* **2007**, *129*, 10575.
[22] W. Känzig, M. H. Cohen, *Phys. Rev. Lett.* **1959**, *3*, 509.
[23] E. Giamello, P. Ugliengo, E. Garrone, *J. Chem. Soc. Faraday Trans. 1* **1989**, *85*, 1373.
[24] E. Giamello, D. M. Murphy, E. Garrone, A. Zecchina, *Spectrochim. Acta* **1993**, *49A*, 1323.
[25] M. C. Paganini, M. Chiesa, E. Giamello, S. Coluccia, G. Martra, D. M. Murphy, G. Pacchioni, *Surf. Sci.* **1999**, *421*, 246.
[26] D. M. Lindsay, D. R. Herschbach, A. L. Kwiram, *Chem. Phys. Lett.* **1974**, *25*, 175.
[27] L. Astrakas, G. Kordas, *J. Chem. Phys.* **1999**, *110*, 6871.
[28] J. Petersen, C. Gessner, K. Fisher, C. J. Mitchell, D. J. Lowe, W. Lubitz, *Biochem. J.* **2005**, *391*, 527.
[29] R. R. Smardzewski, L. Andrews, *J. Chem. Phys.* **1972**, *57*, 1327.
[30] M. Gutjahr, R. Bottcher, A. Pöppl, *Appl. Magn. Reson.* **2002**, *22*, 401.
[31] M. Chiesa, M. C. Paganini, E. Giamello, D. M. Murphy, C. Di Valentin, G. Pacchioni, *Acc. Chem. Res.* **2006**, *39*, 861.
[32] A. Pöppl, L. Kevan, *J. Phys. Chem. B* **1997**, *101*, 3387.
[33] O. Diwald, E. Knözinger, *J. Phys. Chem. B* **2002**, *106*, 3495.
[34] M. Chiesa, E. Giamello, M. C. Paganini, Z. Sojka, D. M. Murphy, *J. Chem. Phys.* **2002**, *116*, 4266.
[35] G. Pacchioni, A. M. Ferrari, E. Giamello, *Chem. Phys. Lett.* **1996**, *255*, 58.
[36] V. Barone in *Recent Advances in Density Functional Methods* (Ed.: D. P. Chong), World Scientific Publishing, Singapore **1996**, p. 278.

Received: March 2, 2010